3637

Liquid Like Solids: A promising, novel multicompartment diffusion MRI phantom material

Courtney J Comrie[1], Malcolm Barrios[1], Isabella Aguilera Cuenca[2], Alexander J McGhee[1], Jindi Sun[1], Shang Song[1,3,4], and Elizabeth B Hutchinson[1]
[1]*Biomedical Engineering, University of Arizona, Tucson, AZ, United States,* [2]*Optical Sciences, University of Arizona, Tucson, AZ, United States,* [3]*Neuroscience, University of Arizona, Tucson, AZ, United States,* [4]*Materials Science and Engineering, University of Arizona, Tucson, AZ, United States*

Synopsis

Keywords: Phantoms, DWI/DTI/DKI, multicompartment phantom, diffusion phantom

Motivation: Traditional single-compartment phantoms lack control over pore size, are more indicative of water restriction, and have limited biological relevance.

Goal(s): Evaluate liquid-like solids (LLS) as a potential dual-compartment phantom material for dMRI.

Approach: LLS phantoms, prepared with different gel concentrations, were imaged with b=0-2500s/mm^2 and the signal curves were compared with free water and silica gel, a restricted phantom material. Additionally, several frameworks were evaluated for multi-compartment dependence.

Results: LLS phantoms show double-exponential DWI signal decay and gel concentration correspondence with dMRI-estimated volume fraction, with Gaussian and non-Gaussian frameworks showing measurable bias, supporting this material's utility in refining multicompartment models.

Impact: Developing biologically relevant multicompartment materials as phantoms can support the advancement of dual tensor and compartment imaging models, allowing innovation and development in more sophisticated diffusion imaging techniques.

Introduction

Developing, optimizing and validating diffusion MRI (dMRI) frameworks for biomedical applications requires phantom materials that resemble biologic tissues. While conventional phantoms such as uniform diffusivity chemical solutions[1], or restricted pore phantoms (e.g. rocks, polystyrene beads) have historically been used for isotropic dMRI validation[2,3]. However, these phantoms lack control over pore size, are primarily more indicative of water restriction, and may not have biological relevance due to the lack of multi-compartments which are present within tissue environments. Liquid-like solids (LLS) originally developed as a 3D cellular matrix are designed to be uniform, aqueous gels composed of evenly sized beads, offering precise control over pore size[4]. This dual-compartment material more closely mimics biological environments, providing freely diffusing and compartmentalized water spaces (figure 1). With these material properties, LLS phantoms offer a novel and promising solution for validating dMRI techniques, especially as more advanced mapping and acquisition techniques progress and develope.

Methods

The phantoms were prepared by heating a mixture of acrylamide (8%), methacrylic acid (2%), poly (ethylene glycol) diacrylate (1%) and azobisisobutyronitrile (0.1%) in ethanol at 70°C. The sample was collected via vacuum filtration, washed with ethanol, and dried in a vacuum oven at 50°C until white solids formed. The resulting gel beads were mixed with water using w/v% to achieve the phantom concentrations of 2%, 6%, 8%, 10%, 12%, 14% and 18%. An additional reference phantom was made from silica gel mixed submerged in water. Standard brightfield digital images were acquired in the 14% phantom concentration using a 50x magnification lens. The phantoms were placed in 0.75 ml glass tubes alongside an additional reference water phantom, and imaged on a 7T Bruker Biospec Scanner. The MRI bore temperature was measured to be 18.07°C. Multi-shell diffusion weighted images were acquired with a 2D spin echo acquisition with TR = 5000 ms, TE = 36 ms, and a spatial resolution of 0.5 x 0.5 with 2-micron slices. Resulting with 186 DWIs with bvalues (directions) = 150 (6), 300 (12), 600 (24), 1200 (48), and 2400 (96) s/mm^2. Diffusion pre-processing, dual-tensor imaging (DT-DTI)[5,6], and mean apparent propagator (MAPMRI)[7] mapping were performed using TORTOISEv4[8]. Based upon ambient temperature the diffusivity of free water was calculated to be 1920 mm2/s for the DT-DTI mapping. The mean signal diffusion kurtosis imaging (MSDKI) model[9,10] was applied via the DIPY Python library on the processed data. Lastly, same sized ROIs were taken of each phantom in ITK-Snap. DWIs of a given bvalue were averaged together, normalized with the amplitude image (silica gel phantom normalized with B0 image), and the ROI voxels of each bvalue were averaged and plotted in MATLAB. Additionally, ROI analysis of metric maps was conducted in MATLAB, where the masked data was averaged and subsequently plotted.

Results

High quality DT-DTI, MAPMRI, and MSDKI maps were obtained (Figure 2) within all LLS phantom concentrations. The DWIs showed an expected exponential signal decay with increasing b-values (Figure 3) and demonstrated higher signal retention in LLS phantoms with increasing gel concentrations when compared to the reference water phantom. In contrast, the silica gel phantom displayed a differing decay rate pattern. Figure 4 confirmed an increasing volume fraction with higher LLS concentrations. Increasing values were observed in MAPMRI and DT-DTI return-to-origin propagators (RTOP), mean signal kurtosis (MSK), and non-Gaussianity (NG), while mean signal diffusivity (MSD) decreased. Gel compartment diffusivity (GCD) remained similar across the final 5 LLS concentrations.

Discussion

The results depict that dual-compartment LLS phantoms are promising for biologically relevant dMRI validation. The DWI signal decay in LLS phantoms follows a predictable pattern across gel and water concentrations. This contrasts with the silica gel phantom, which exhibits a distinct decay trajectory diverging away during the early bvalue stages. The similar GCD values at higher concentrations suggest a fixed gel diffusivity, distinct from the free water compartment, with an average value of 2625 μm^2/s as shown in Figure 1. The observed increase in NG with respect to LLS concentrations likely reflects the increasing presence of multiple compartments within the medium.

Conclusion

Characterization of these phantoms after separation of free water, provided the identification of GCD, and observed increasing NG supporting due the presence of a multi-compartment structure LLS materials, as dMRI dual-compartment phantoms, more accurately mimic biological environments than traditional single-compartment phantoms.

Acknowledgements

This research was supported by NIA/NIH grant R01AG07928 and by the National Institute of Aging of the National Institutes of Health under award number T32AG082631-01. All imaging was performed in the UA translational bioimaging resource (TBIR) and made possible by the NIH small instrumentation grant: S10 OD025016. The authors would like to thank High Performance Computing (HPC) for providing the resources needed. Thank you to all the MBSIL members for their support.

Figures

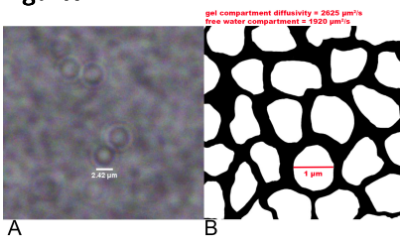

Figure 1. A) Brightfield image of single gel bead in the 14% liquid like solid (LLS) concentration taken at 50x with a 2.42-micron diameter. B) Illustration of gel compartments with free water in between the theoretical 1-micron sized beads. Gel compartment diffusivity and free water compartment reported above at 2625 μm^2/s and 1920 μm^2/s respectively.

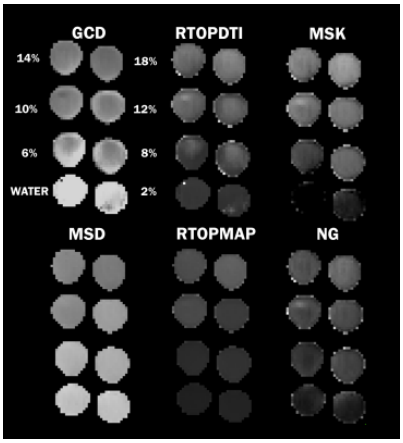

Figure 2. Overview of the following metric maps analyzed in this abstract: gel compartment diffusivity (GSD), return-to-origin probability via dual tensor imaging (RTOPDTI), mean signal kurtosis (MSK), mean signal diffusivity (MSD), return-to-origin probability via mean apparent propagort (RTOPMAP), and non-gaussianity (NG). Along with reported gel concentrations following the same pattern, indicated in GSD for all other maps.

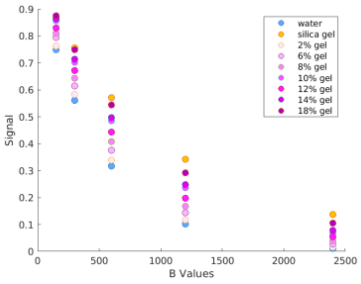

Figure 3. Diffusion weighted images' signal with respect to increasing bvalues for all gel concentrations (darkening pink gradient for increasing concentrations), water (blue), and silica gel phantom (yellow).

References

1. C. Pierpaoli, J.S., U. Nevo, P. J. Basser, and F. Horkay, Polyvinylpyrrolidone (PVP) water solutions as isotropic phantoms for diffusion MRI studies Proc. Intl. Soc. Mag. Reson. Med., 2009.
2. Callaghan, P.T., et al., Diffraction-Like Effects in Nmr Diffusion Studies of Fluids in Porous Solids. Nature, 1991. 351(6326): p. 467-469.
3. Benjamini, D., et al., Nonparametric pore size distribution using d-PFG: Comparison to s-PFG and migration to MRI. Journal of Magnetic Resonance, 2014. 246: p. 36-45.
4. Bhattacharjee, T., et al., Liquid-like Solids Support Cells in 3D. Acs Biomaterials Science & Engineering, 2016. 2(10): p. 1787-1795.
5. Williamson, N.H., et al., Real-time measurement of diffusion exchange rate in biological tissue. Journal of Magnetic Resonance, 2020. 317.
6. C. Pierpaoli, D.K.J., Removing CSF Contamination in Brain DT-MRIs by Using a Two-Compartment Tensor Model Proc. Intl. Soc. Mag. Reson. Med., 2004.
7. Ozarslan, E., et al., Mean apparent propagator (MAP) MRI: a novel diffusion imaging method for mapping tissue microstructure. Neuroimage, 2013. 78: p. 16-32.
8. Irfanoglu, M.O., TORTOISE v3: Improvements and New Features of the NIH Diffusion MRI Processing Pipeline. 25th Annual Meeting of the International Society fro Magnetic Resonance, 2018.
9. Jensen, J.H., et al., Diffusional kurtosis imaging: the quantification of non-gaussian water diffusion by means of magnetic resonance imaging. Magn Reson Med, 2005. 53(6): p. 1432-40.
10. Henriques, R.N., et al., Diffusional Kurtosis Imaging in the Diffusion Imaging in Python Project. Front Hum Neurosci, 2021. 15: p. 675433.

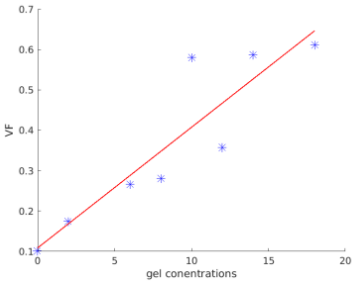

Figure 4. Separated volume fraction (VF) of liquid-like solids for all phantom concentrations imaged.

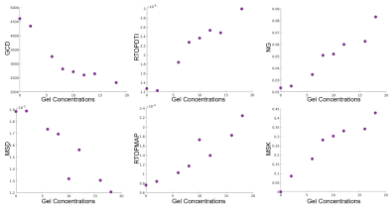

Figure 5. Quantitative analysis of the metric map values according to the liquid like solids (LLS) gel concentrations. The maps are as follows starting at the top-right to the bottom-left: gel compartment diffusivity (GCD), return-to-origin probability via dual tensor imaging (RTOPDTI), non-guassianity (NG), mean signal diffusivity (MSD), return-to-origin-probability via mean apparent propagator (RTOPMAP), and mean signal kurtosis (MSK).